Improvement of pea protein gelation at reduced temperature by atmospheric cold plasma and the gelling mechanism study

Sitian Zhang [1], Weijuan Huang [1], Ehsan Feizollahi, M.S. Roopesh [*], Lingyun Chen [*]

Department of Agricultural, Food & Nutritional Science, University of Alberta, Edmonton, Alberta T6G 2P5, Canada

A B S T R A C T

Pea protein as an alternative of soy protein has attracted growing interest in food industries. However, high temperature (> 95 °C) is required to enable heat-induced gelation and the formed gels are relatively weak. This research aimed to study the efficacy of atmospheric cold plasma (ACP) as a novel non-thermal technique to improve the gelling properties of pea protein. While native pea protein concentrate (PPC) (12 wt%) could not form gel under 90 °C, ACP-treated PPC showed good gelling properties when heated at 70–90 °C. The gels exhibited homogeneous three-dimensional network structure with interconnected macropores, and those prepared at 80 and 90 °C possessed good mechanical strength and viscoelasticity, as well as high water holding capacity. The gelling mechanism was studied by monitoring pea protein structural changes during ACP treatment and gel formation process via a transmission electron microscope, a Fourier transform infrared spectrometer, and a rheometer. These results revealed that ACP treatment contributed to the formation of protein fibrillar aggregates, and significantly reduced the PPC denaturation temperature, leading to protein unfolding at reduced temperature of 80–90 °C. ACP treatment also increased the protein surface hydrophobicity and exposed free sulfhydryl groups, which could facilitate the formation of hydrophobic interactions and disulfide bonds, leading to gels with improved mechanical properties. Moreover, hydrogen bonding could play an important role to stabilize the gel network during the gelling process. Owing to the short exposure time and energy efficiency, ACP is a promising technology to enable wide applications to pea protein as a gelling ingredient of plant protein-based food products, such as meat analogues and egg alternatives.

1. Introduction

Atmospheric cold plasma (ACP) as a novel non-thermal technology, has gained attention as a potential alternative to traditional thermal processing for microbial inactivation to extend the shelf life of different food products (such as fruits, vegetables, meats, eggs, and cereals) (Miao et al., 2020). ACP technology has the advantages of shorter treatment time and no thermal damages to food physical properties (e.g., color, texture), flavors and nutritive components (e.g., vitamins and flavonoids) due to its lower temperature (< 60 °C) compared to traditional thermal processing (Deng et al., 2007; Mandal, Singh, & Singh, 2018). At atmospheric pressure, when air is used, ACP process generates two main reactive species, including reactive oxygen species (ROS) (O₃, O, O^-, O_2^-, O_2^{2-}, H_2O_2 and ·OH) and reactive nitrogen species (RNS) (NO, NO_2 and N_2). These species can trigger the lipid peroxidation in microbial cell membranes, and oxidize proteins and DNA, leading to

microbial inactivation (Feizollahi, Misra, & Roopesh, 2020). The active species generated by ACP can also break covalent bonds and initiate some chemical reactions (Kim, Lee, & Min, 2014). Thus, ACP has the potential to be used for protein modifications.

Recently, ACP technology has been applied to modify protein structures. ACP treatment improved the solubility and functions of peanut protein and zein in recent research works (Dong et al., 2017; Ji et al., 2018). This is because high-energy reactive species could induce the etching reaction to expose the active sites on protein surface, which increases the affinity between protein and water molecules. The enhanced surface polarity of the protein molecules by ACP treatment is associated with the improved solubility (Dong, Gao, Xu, & Chen, 2017; Ji et al., 2018; Ji et al., 2019). In addition, ACP technology could affect the formation of disulfide bonds in proteins, leading to improved foam stability of whey protein and enhanced dough strength of wheat glutenin (Bahrami et al., 2016). More recently, Dong et al. (Dong et al.,

2018; Dong, Wang, et al., 2017) found that the surface hydrophilicity, flexibility, and tensile strength of zein film were improved after ACP treatment.

Consumers are increasingly interested in dietary intake of plant proteins due in part to health, sustainability, and ethical concerns. Canada is the world's second-largest pea (*Pisum sativum, L.*) producer with an annual dry pea production of 3.6 million metric tons (Bard, 2019). Protein accounts for 22–25% in dry pea seeds (Tayeh et al., 2015). Globulins are dominant in pea protein with legumin (11S), vicilin, and convicilin (7S) as the main fractions (Ben-Harb et al., 2018). Legumin is a hexamer (350–400 kDa) consisting of acidic and basic subunits linked by disulfide bonds (–S–S–), and each legumin subunit contains up to seven cysteine and four methionine residues. Vicilin (~170 kDa) contains three subunits of ~50 kDa, but no cysteine and a few methionine residues. Convicilin is a protein with a molecular weight of 280 kDa, consisting of 4–10 kDa subunits (Croy, Gatehouse, Tyler, & Boulter, 1980). Pea protein is a good alternative to soybean protein due to its high nutritional value and hypoallergenic status. Nowadays, pea protein concentrates and isolates are used as food supplements for athlete diets and functional ingredients in food formulations due to their functional properties (Moreno et al., 2020).

Gelation is one of the most important functional properties of globular proteins. Proteins form hydrogels through physically or chemically crosslinking between polypeptide chains that trap a large amount of water within their three-dimensional network to tailor food texture (Abaee, Mohammadian, & Jafari, 2017). Pea proteins also show gelling properties, but previous works reported that the pea protein gels were weaker and less elastic than soy protein gels, which limited their applications in food industries (Shand, Ya, Pietrasik, & Wanasundara, 2007). Less disulfide bonds were formed in pea legumin gels due to limited cysteine than that in soybean glycinin (12S fraction) and disulfide bonds are known to strengthen protein gel networks (O'Kane, Vereijken, Gruppen, & Van Boekel, 2005). Besides, high temperature heating is required to induce pea protein gelation (95 °C) due to their high denaturation temperature (> 85 °C) (Liang & Tang, 2013), which may place a hurdle for pea protein application in food products as a gelling ingredient, since the internal temperature is generally 75 °C when food is cooked (Health and Human Services, 2017). Given that, ACP technology can improve the solubility of protein, expose active groups, and promote disulfide bonds formation in protein molecules, it was hypothesized that pea protein gelling properties could be improved by ACP treatment. Until now, only one research reported that ACP was able to modify the structure and techno-functional properties of pea protein including solubility, water and fat binding capacities (Bußler, Steins, Ehlbeck, & Schlüter, 2015). There is no report yet regarding the impact of ACP pre-treatment on pea protein gelling properties.

This research aimed to study ACP as a pre-treatment technology to improve pea protein gelling properties. Pea protein concentrate (PPC) suspension was treated by ACP technology. The gelling properties of ACP-treated PPC gel that were formed at different temperatures (70, 80, and 90 °C) were studied. The gel microstructures, mechanical and rheological properties, and the water holding capacity were determined. The protein structural changes and the gel formation mechanisms of PPC treated by ACP technology were investigated. Proving of the hypothesis will provide a new strategy to broaden the application of pea protein as a gelling ingredient in food formulations, such as meat binder and fat replacer, to create food with improved quality and nutritive value.

2. Materials and methods

2.1. Materials and chemicals

Pea protein powder (53.1% protein, 33.7% carbohydrate, 2.0% fat, 5.3% ash, and 5.9% moisture) was provided by AGT Foods Research & Innovation Centre (Saskatoon, SK, Canada) and used as the raw material to obtain pea protein concentrate. Sodium dodecyl sulfate (SDS), 2-mercaptoethanol (2-ME), 5,5′-dithiobis-(2-nitrobenzoic acid) (DTNB), 1-anilinonaphthalene-8-sulfonic acid (ANS), 2,4,6-trinitrobenzene sulfonic acid (TNBS) (5% (*w/v*) in H$_2$O), glycine, L-lysine, Trizma® base and ethylenediaminetetraacetic acid (EDTA) were purchased from Sigma-Aldrich (St. Louis, MO, USA), urea and other chemicals (analytical grade) were purchased from Fisher Scientific (Fair Lawn, NJ, USA).

2.2. Preparation of pea protein concentrate (PPC)

PPC was prepared as described by Walia and Chen (2020) with minor modifications. Briefly, pea protein powder was mixed with distilled water at a 1:7 ratio (w/v) and the pH of the suspension was adjusted to 9 using 1 M NaOH. After stirring for 1 h at room temperature, the mixture was centrifuged at 8000 ×g for 15 min (Acanti® J-E centrifuge, Beckman Coulter, USA). The supernatant was collected and adjusted to pH 4.5 using 1 M HCl. Then the suspension was centrifuged at 8000 ×g for 15 min and the precipitate was collected. The pellet was dispersed in distilled water and adjusted to pH 7 by adding 1 M NaOH. Next, the mixture was dialyzed (3.5 kDa MWCO dialysis tubing) against distilled water for three days and then lyophilized to obtain the PPC powder. The protein content was 87.2% measured by a Leco nitrogen analyzer (Leco®, USA) using a nitrogen-to-protein conversion factor of 5.96 (Fujihara, Kasuga, & Aoyagi, 2001).

2.3. Atmospheric cold plasma (ACP) treatment

ACP with a dielectric barrier discharge plasma system (PG 100–D, Advanced plasma solutions, Malvern, USA) was used to treat the PPC sample. Pea protein suspension (12 wt%) was prepared by dispersing pea protein power (1.2 g) in distilled water (8.8 g) with magnetic stirring (700 rpm) at room temperature (22–23 °C) for 2 h and then stirred overnight at 4 °C in a refrigerator to ensure thorough hydration. In the next day, the PPI suspension was taken out from the fridge (4 °C) to return to room temperature before further experiments. Approximate 2 mL of 12 wt% PPC suspension in a 4-cm diameter and 0.5-cm height plastic container (METER®, Pullman, WA, USA) was placed between a high-voltage electrode and a ground electrode. The distance from the sample surface to the high-voltage electrode was maintained at 2 mm, the frequency was 3500 Hz and the duty cycle was 70%. The voltage output was 0–30 kV, the current output was 0–1 A, and the pulse width was 10 μs. The sample was treated for 2 min, followed by well stirring. This process was repeated five times, so the total treatment time was 10 min. The temperature of ACP-treated sample was increased from 21.3 °C to 23.5 °C.

2.4. Preparation of PPC gels

Approximately 5 mL of ACP-treated PPC (12 wt%, pH 6.0) was adjusted the pH to 6.9 and then transferred into a 10 mL (BPA-free) of cryovial (Simport polypropylene T310-10A) at room temperature. All tubes were centrifuged at 3000 ×g for 1 min (Centrifuge 5810 R, Eppendorf, Germany) to remove air bubbles, and then they were heated at 70, 80, and 90 °C for 30 min followed by cooling in an ice-water bath for 10 min, and then stored in a fridge (4 °C) for 24 h prior to analysis. The gels were also prepared from untreated PPC suspension (pH 6.9) at the same concentration and temperature for comparison. Each sample was replicated three times.

2.5. Mechanical properties of PPC gels

Mechanical properties of gel samples were measured using an Instron 5967 universal testing instrument (Instron Corp., MA, USA) equipped with a 50 N load cell (Yang, Wang, Vasanthan, & Chen, 2014). The gel samples had a height of 8 mm and a diameter of 14 mm. The sample was compressed to 30% of its original height with a rate of 1 mm/min at room temperature (22–23 °C). Compressive strength was calculated as

the maximum compressive stress in the stress-strain curve. Young's modulus was determined by the slope of the linear section (the compressive strain of 0–10%) in the stress-strain plots.

2.6. Rheological measurements

Rheological measurements were performed on a TA Discovery HR-3 rheometer (TA Instruments, DE, USA) using a parallel plate geometry with a diameter of 40 mm. Unless described otherwise, all measurements were conducted at a gap of 1 mm by applying a constant strain of 1%. Frequency sweeps were done to determine the storage modulus G' and loss modulus G" at oscillation frequency from 0.1 to 100 rad/s. To study the changes in viscoelastic properties as a function of temperature, the PPC suspensions with or without APC treatment were subjected to a temperature ramp at a rate of 2 °C/min from 25 to 90 °C, held at 90 °C for 30 min, and then cooled down to 4 °C, and held at 4 °C for 30 min. Silicone oil was applied to cover the surface of samples to prevent evaporation during the tests. There was no sample weight loss before and after the tests and the effect of silicone oil on the measurements was regarded as negligible. The temperature of the plate was controlled with a Peltier system. All rheological measurements were performed within a predetermined linear viscoelastic region at the strain value at 1%.

Molecular interactions involved in the gel formation were studied by a rheological measurement in presence of dissociation reagents (Nieto-Nieto, Wang, Ozimek, & Chen, 2015) with some modification. The gel samples were cut into approximately a height of 1.0 cm and a diameter of 1.4 cm. The resulting gel disks were immersed into 0.6 M 2-mercaptoethanol (2-ME), 6 M urea, or 3% (w/v) sodium dodecyl sulfate (SDS) solution for 48 h at room temperature. The gel disks immersed in the distilled water were used as control samples. A frequency sweep analysis was conducted on the soaked gels to measure G' and G".

2.7. Water holding capacity (WHC) of PPC gels

Water holding capacity (WHC) was determined according to a method described by Nieto-Nieto, Wang, Ozimek, and Chen (2016) with slight modification. PPC gel samples (1.0 g) were placed into a Vivaspin 20 centrifugal filter unit (GE Healthcare Bio-Sciences AB, Uppsala, Sweden) and centrifuged at 4000 ×g for 20 min. The weight of the gel was recorded before or after centrifugation. The WHC of gels was calculated according to eq. (1):

$$WHC = \frac{M_1 - M_2}{M_1} \times 100\% \tag{1}$$

Where M_1 represents the mass of total water in the gel before centrifugation (g), M_2 represents the mass of water released in the gel by centrifugation (g).

2.8. Morphology of PPC gels and PPC suspensions

The morphology of protein samples before or after ACP treatment in suspension was observed using a transmission electron microscope (TEM, Morgagni 268, Philips-FEI, Hillsboro, USA) at an accelerating voltage of 80 kV. A drop of the diluted PPC suspensions (0.03 wt%) was transferred onto a carbon film-covered 400 mesh copper grid for 45 s. Subsequently, a drop of 4% uranyl acetate (staining solution) was added for negative staining for 5 s, then the excess solution was removed with filter paper.

A Zeiss EVO M10 scanning electron microscope (SEM) (Carl Zeiss AG, Oberkochen, Germany) was used to examine the microstructure of the PPC gels. The gel samples were rapidly frozen in liquid nitrogen, and then freeze-dried. The cross-sections of the gel samples were sputter-coated with gold under vacuum for 90 s and then was observed to record the microstructure at 20 kV.

2.9. Surface charge

The surface charge (zeta potential) of PPC suspensions with or without ACP treatment were determined by laser Doppler velocimetry using a Zetasizer Nano-ZS (Malvern Instruments Ltd., UK). The protein refractive index (RI) was set at 1.45 and dispersion medium RI was 1.33. The samples were properly diluted before measurement.

2.10. Content of free sulfhydryl (−SH) and free amino (−NH_2) groups

The contents of free −SH groups including total and exposed −SH were measured using the method described by Dong, Gao, et al. (2017) with modification. PPC suspensions (12 wt%) with or without ACP treatment were diluted five times with Tris-glycine buffer (pH 8.0). Then 1.0 mL of the diluted sample suspension was mixed with 2.0 mL of Tris-glycine buffer (pH 8.0) and 0.02 mL of Ellman's reagent (DTNB, 5,5′-dithiobis-(2-nitrobenzoic acid), 4.0 mg/mL) in 5.0 mL of microcentrifuge tubes. After the mixture was incubated at 25 °C for 5 min, the exposed free −SH group content was determined at 412 nm using a SpectraMax M3 microplate reader (Molecular Devices, USA). The total −SH group content was evaluated as well. First, 0.5 mL of diluted samples was mixed with 0.05 mL of 2-mercaptoethanol and 2.5 mL of 10 mol/mL urea in Tris-glycine buffer (pH 8.0) in 15 mL centrifuge tubes. After incubating at 25 °C for 1 h, 2.5 mL of 12% trichloroacetic acid (TCA) was added and the mixture was further incubated for 1 h at 25 °C. Subsequently, the tubes were centrifuged at 3000 ×g for 15 min and the precipitate was suspended in 2.0 mL of 12% TCA. The mixture was centrifuged again to remove the 2-mercaptoethanol. Finally, the precipitate was dissolved in 3.0 mL of 8.0 mol/mL urea in Tris-glycine buffer (pH 8.0) and then 0.05 mL Ellman's reagent was added. After 5 min, the absorbance was read at 412 nm using a SpectraMax M3 microplate reader (Molecular Devices, USA). The content of the free −SH group was calculated according to eq. (2).

$$SH\left(\frac{\mu mol}{g}\right) = \frac{73.53 \times A \times D}{C} \tag{2}$$

Where A is the absorbance at 412 nm; D is the dilution multiple; C is the sample concentration (mg/mL).

The content of free −NH_2 groups was evaluated by the trinitrobenzene sulphonate (TNBS) assay (Habeeb, 1966) with slight modification. The PPC suspensions with or without ACP treatment were diluted with reaction buffer (0.1 M sodium bicarbonate, pH 8.5). And 0.01% (w/v) TNBS solution was prepared using reaction buffer as the diluent. Then, 0.5 mL of the sample was mixed with 0.25 mL of the 0.01% TNBS solution. After incubating at 37 °C for 2 h, 125 μL of 1 N HCl was added to the mixture to terminate the reaction. Then the absorbance of the mixture was recorded at 335 nm using a SpectraMax M3 microplate reader (Molecular Devices, USA). L-lysine solution (2.5, 5, 10, 20, and 40 μg/mL) was used as a standard instead of a sample to repeat the above experimental steps and record absorbance. The content of free −NH_2 groups was calculated by the standard curve.

2.11. Surface hydrophobicity (H_0)

The surface hydrophobicity (H_0) of samples was evaluated using the fluorescent probe 1-anilinonaphthalene-8-sulfonic acid (ANS) (Kato & Nakai, 1980) according to Chalamaiah, Esparza, Temelli, and Wu (2017) with slight modification. Serial dilutions (protein concentration of 0.001 to 0.5 mg/mL) of the PPC suspensions with or without ACP treatment were prepared by diluting with 0.1 M phosphate buffer (pH 7.4). Then, 20 μL of 8 mM ANS solution was mixed with 4 mL diluted sample. The fluorescent intensity was measured at an excitation wavelength of 390 nm and an emission wavelength of 460 nm using a SpectraMax M3 microplate reader (Molecular Devices, USA) after the mixture was kept in the darkroom for 15 min. The initial slope of the corrected

fluorescence intensity (the fluorescence intensity of protein suspension with ANS subtracted protein suspension without ANS) versus protein concentration plot was calculated by linear regression analysis and used as an index of surface hydrophobicity.

2.12. Protein secondary and tertiary structural change

FTIR spectra of the PPC in suspensions and gels were recorded using a Nicolet 6700 Fourier transform infrared spectrophotometer (Thermo Fisher Scientific Inc., MA, USA). All data were collected in the spectral range from 4000 to 800 cm^{-1} during 128 scans at a spectral resolution of 4 cm^{-1}. D$_2$O was used as a solvent for the PPC suspensions and gels preparation. The samples were placed between two CaF$_2$ windows separated by a 25 μm polyethylene terephthalate film spacer for test. The spectrophotometer was continuously purged with dry air from a lab gas generator (Parker Hannifin Corp., USA). Protein secondary structures (α-helices, β-sheets, β-turns, and random coils) were determined by analyzing the amide I band region (1700–1600 cm^{-1}) according to the Fourier self-deconvolution (FSD) algorithm using Omnic 8.1 software (Thermo Fisher Scientific, MA, USA) at a bandwidth of 24 cm^{-1} and an enhancement factor of 2.5.

The fluorescence spectra of the PPC suspensions with or without ACP treatment were measured by a SpectraMax M3 microplate reader (Molecular Devices, USA). The samples were properly diluted before measurement. The excitation wavelength was 295 nm. The emission spectra at 300–400 nm were recorded at 10 nm/s scanning speed. The emission and excitation slits were set at 3 nm.

2.13. Statistical analysis

All experiments were performed in three independent batches and the data were reported as mean ± standard deviations. Statistical evaluation was analyzed using a paired *t*-test or One-way analysis of variance followed by *post-hoc* test (Fisher's Least Significant Difference (LSD)). All of the analyses were conducted using SPSS 21.0 software (IBM Corp., USA) with a probability of $p < 0.05$ considered to be significant.

3. Results and discussion

3.1. Properties of gels prepared from PPC with ACP treatment

3.1.1. Mechanical properties and water holding capacity

In preliminary trials, the impact of various ACP treatments on pea protein properties was studied, and the optimized condition (3500 Hz, 10 μs, 10 min, 0–30 kV, and 0–1 A) can efficiently improve the gelling capacity. The photos in Fig. 1A display the gels formed with ACP-treated and untreated PPC suspensions (12 wt%) heated for 30 min at 70, 80, and 90 °C, respectively. The native PPC suspension (12 wt%) could not form a gel after heating at 100, 110, and even 120 °C for 30 min. Even though the protein concentration was increased to 15 wt%, a very weak gel was formed after heating at 95 °C for 30 min, no gels were formed at temperature below 95 °C. However, the PPC suspension after ACP treatment formed gels even at 70 °C, which was significantly lower than the denaturation temperature (legumin of around 92 °C) of pea protein (Liang, et al., 2013). Fig. 1A and B show the impact of heating on the mechanical properties of the gels formed from ACP-treated PPC. The gel formed at 70 °C showed a compressive strength of 0.53 kPa, and this value increased to 2.70 kPa and 6.27 kPa when the temperature was raised to 80 °C and 90 °C, respectively. The Young's modulus of the gel formed at 90 °C was 5.84 kPa, followed by gel heated at 80 °C (4.21 kPa) and 70 °C (1.43 kPa). It was noted that the gels formed at 80 °C from 12 wt% ACP-treated PPC showed even higher mechanical strength than those of native pea protein gels (15 wt%) heated at 95 °C for 30 min
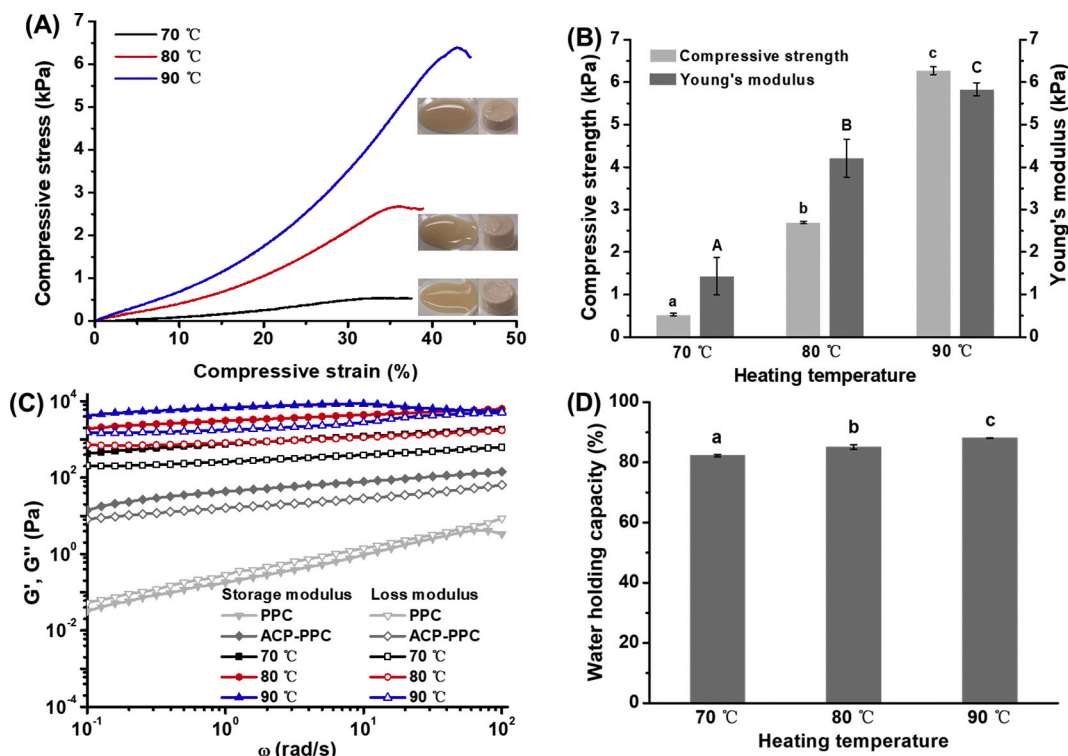

Fig. 1. Mechanical properties and water holding capacity of pea protein concentrate (PPC) gels made from PPC suspension treated by atmospheric cold plasma (ACP) (12 wt%; Treated conditions: 3500 Hz, 10 μs, 10 min, 0–30 kV, and 0–1 A) heated at different temperatures (70, 80, and 90 °C) for 30 min. (A) Typical compressive stress-strain curves and photographs of corresponding gels (Left: Untreated PPC gels; Right: ACP-treated PPC gels). (B) Compressive strength and Young's modulus values of gels. (C) Frequency dependence of storage modulus (G') and loss modulus (G") of PPC suspensions and gels. (D) Water holding capacity of PPC gels. Different letters represent significant differences (p < 0.05).

(1.03 kPa) (Munialo, van der Linden, & de Jongh, 2014). In addition, The Young's modulus of the gel formed by ACP-treated PPC at 80 °C for 30 min (4.21 kPa) was higher than that of the gel formed by soy protein isolate (15 wt%, pH 7, 10 mM CaCl$_2$) at 80 °C for 30 min (1.84 kPa) (Brito-Oliveira, Bispo, Moraes, Campanella, & Pinho, 2018).

Water holding capacity of a gel is an important property for its application in food production because a lack of water has a negative impact on the texture and quality of a foodstuff. Fig. 1D demonstrates good water holding capacity (80–90%) of the gels prepared at all the tested temperatures, which was comparable or even slightly higher than soy protein gels (50–80%) (Braga, Azevedo, Marques, Menossi, & Cunha, 2006; Brito-Oliveira et al., 2018; Tsumura et al., 2005).

3.1.2. Viscoelastic properties

The storage modulus (G') and loss modulus (G'') indicate the elastic and viscous properties of gels. As shown in Fig. 1C, G'' > G' was observed for native PPC in suspension, indicating liquid behavior dominated in the sample. While G' > G'' was observed for ACP-treated PPC suspension along with an almost constant G' at all frequencies tested, implying a weak gel behavior for pea protein after ACP treatment (Ben-Harb et al., 2018). But G''-value of ACP-treated PPC suspension shows a high dependence on frequency from 10^{-1} to 10^2 rad/s, suggesting formation of the entanglement networks which were formed by the simple topological interaction of polymer chains rather than by cross-linking (Picout & Ross-Murphy, 2003). Thus, PPC suspension treated with ACP did not form the solids "true" gels, but structured fluids. The G' was higher than G'' of the gel samples, indicating that all samples exhibited solid-like behaviors. Both moduli increased with increasing the heating temperature, which indicated that the formed gel became stronger as the heating temperature increased. Higher heating temperature led to an increased degree of protein unfolding, thus more active groups were exposed to facilitate covalent and non-covalent interactions, which brought out stronger three-dimensional gel networks. In addition, the G' of the gel heated at 90 °C decreased sharply when the frequency exceeded around 10 rad/s as a result of gel break down at large deformation, which is a typical behavior of strong gels (Martínez-López et al., 2016). Above rheological characterization results demonstrate structured fluid formed from PPC by APC treatment, which was then converted into viscoelastic gels by heating at 70–90 °C.

3.1.3. Morphology of protein suspensions and gels

As ACP-treated PPC showed solid-like behavior based on rheological results, the morphology of PPC with or without ACP treatment was observed by TEM. As shown in Fig. 2A, the PPC in its native state showed particles larger than 20 nm and it was noted that particles seem to be flocculated. The reason might be due to the drying processing to prepare TEM samples that causes some protein particles to aggregate. As showed in Fig. 2B, fibrillar structure was observed for ACP-treated PPC, indicating the formation of fibrillar aggregates of PPC as a result of ACP treatment.

The microstructures of PPC gels prepared at 70, 80, and 90 °C are shown in SEM images (Fig. 2). The 3D gel network was obtained from PPC even at 70 °C, but relatively loose structure with uneven pores formed from particulate aggregates was observed (Fig. 2C). When the heating temperature was increased to 80 °C, strong 3D gel networks with regular interconnective pores were formed (Fig. 2D). The pores became larger and more homogenous when the gel was formed at 90 °C, showing a macro-porous wall network structure (Fig. 2E). The regular interconnective porous network structure explained the good firmness and elasticity of the PPC gels prepared at 80 and 90 °C, as well as their high water holding capacity because gels with uniform pore structure possess the good capacity to hold moisture through capillary forces (Wu, Xiong, Chen, Tang, & Zhou, 2009).

3.2. PPC structure changes through ACP treatment and during gelling process

3.2.1. Gelation and dissociation of process

Dynamic rheological properties of the PPC suspensions with or without ACP treatment were studied when subject to a temperature ramp to simulate the gelation process (Fig. 3). G' and G'' of ACP-treated PPC suspension were much larger than that of untreated PPC suspension. For untreated PPC suspension, G' was lower than G'' initially, indicating a liquid-like behavior. Both G' and G'' were reduced from 25 °C to 76 °C, likely due to the decrease of hydrogen bonds and electrostatic interactions in protein molecules by initial heating, which resulted in decreased viscosity of the suspensions (Wang et al., 2017). Untreated PPC started to show solid behavior at 76 °C when G' and G'' crossed each other, and the G' value increased from 76 to 90 °C. A continuous increase in G' was observed during holding at 90 °C for 30 min and then in the process of cooling to 4 °C. However, in the actual gelation experiment, the native PPC suspension did not form a gel even when heated at 90 °C for 30 min followed by cooling. This suggests that native PPC continued to develop crosslinking during heating and cooling processing, but the protein concentration and heating temperature was not sufficient for it to form a self-standing gel network. For ACP-treated
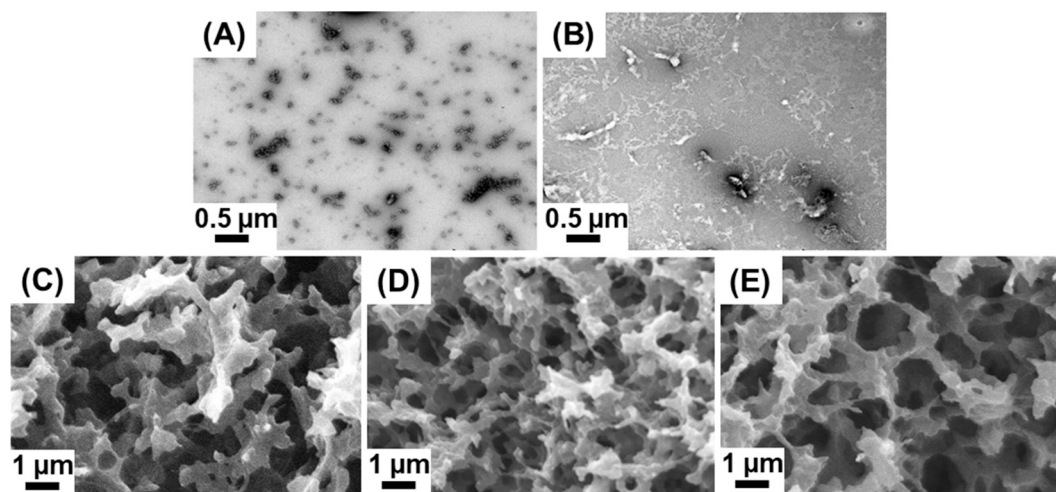

Fig. 2. Transmission electron microscopy (TEM) images of pea protein concentrate (PPC) suspensions with (B) or without (A) atmospheric cold plasma (ACP) treatment. Scanning electron microscopy (SEM) images of PPC gels made from PPC suspension treated by ACP at different heating temperatures for 30 min. (C) 70 °C, (D) 80 °C and (E) 90 °C. ACP treated conditions: 3500 Hz, 10 µs, 10 min, 0–30 kV, and 0–1 A.
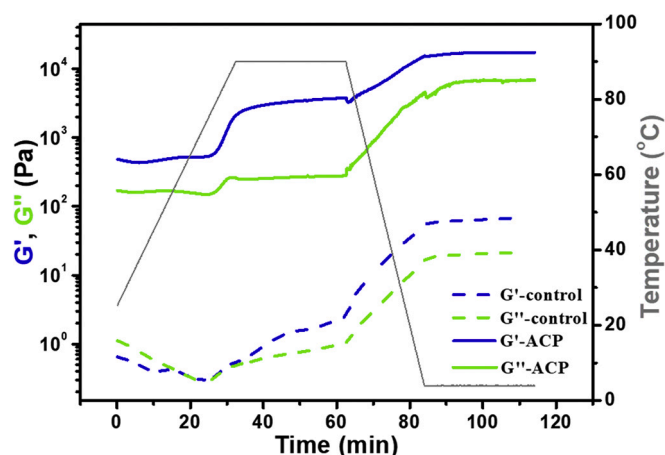
Fig. 3. Effect of simulated gelation process on storage modulus (G') and loss modulus (G") of pea protein concentrate (PPC) suspensions (12 wt%) with or without atmospheric cold plasma (ACP) treatment (3500 Hz, 10 μs, 10 min, 0–30 kV, and 0–1 A) during heating from 25 to 90 °C at a rate of 2 °C/min, holding 30 min at 90 °C, then cooling from 90 to 4 °C at a rate of 4 °C/min and holding 30 min at 4 °C. The temperature is depicted in grey.

PPC suspension, structured fluid was formed before heating as mentioned in section 3.1.2, thus G' was higher than G" at the beginning. A decrease in G' value during heating from 25 °C to 39 °C indicates that the formed protein network structure was interrupted to a certain extend probably due to the breaking of hydrogen bonds at the initial heating step, leading to a loss of firmness. While G' and G" values of ACP-treated PPC suspension maintained consistent with increasing temperature from 39 °C to 75 °C, G' increased sharply from 75 °C to 90 °C, suggesting gelation started at 75 °C. In the second phase when the temperature was maintained at 90 °C for 30 min, G' of ACP-treated PPC suspension remained almost unchanged, suggesting no further gel-enhancement was occurred during the isothermal stage. Next, when the temperature was decreased from 90 °C to 4 °C in the third phase, G' increased sharply, indicating that cooling stage further strengthened the 3D gel network. This might be related to increased hydrogen bonds in the gel network, which is favored at lower temperatures.

In order to further study the interactions involved in the gel formation from ACP treated PPC, the gels formed at 90 °C were immersed into dissociation reagents including urea, sodium dodecyl sulfate (SDS) and 2-mercaptoethanol (2-ME). They were applied to disrupt hydrogen bonds, hydrophobic interactions and disulfide bonds, respectively. As shown in Fig. 4A, the size of the gel after immersing in urea was slightly larger than the gel soaked in water. The gel shrunk after immersing in SDS solution for 48 h. But there was no apparent change in the size of the gel after immersing in 2-ME comparing to the gel soaked in water. In addition, the gels soaked in urea and SDS reagents became translucent, but the gel soaked in 2-ME slightly changed to pale white comparing with gel soaked in water. Fig. 4B shows the rheological properties of gels soaked in dissociation reagents, and the gels soaked in water were also tested for control. G' and G" of gels soaked in urea and SDS solutions were significantly lower than the control group. This result suggests that hydrogen bonding and hydrophobic interactions played important roles to stabilize the gel network along with a small amount of disulfide bonds, because the cysteine content is low in pea protein.

3.2.2. Chemical structural changes

Table 1 summarizes the changes in the surface charge of untreated and ACP-treated PPC suspensions. Since the isoelectric point of pea protein (about pH 4.5) was lower than the pH value of the native PPC suspension (pH 6.9) and the ACP-treated PPC suspension (pH 6.0), both samples were negatively charged as reflected in their zeta potential values. The decrease in pH by ACP treatment might be due to the
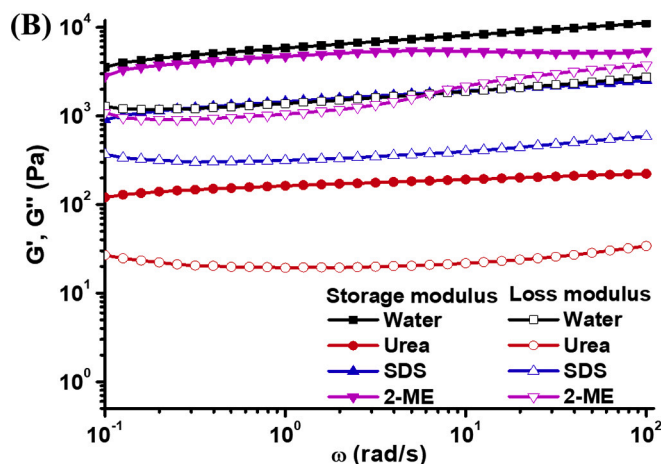

Fig. 4. Gel dissociation results. (A) Photos of pea protein concentrate (PPC) gels after immersing in different dissociation reagents for 48 h. (B) Frequency dependence of storage modulus (G') and loss modulus (G") of PPC gels after immersing in different dissociation reagents for 48 h.

Table 1

Zeta potential of pea protein concentrate (PPC) suspensions with or without atmospheric cold plasma (ACP) treatment (3500 Hz, 10 μs, 10 min, 0–30 kV, and 0–1 A).

Samples	Zeta potential (mV)
PPC suspension	-27.3 ± 0.53[b]
ACP-treated PPC suspension	-24.2 ± 0.10[a]

Different lower-case letters within a column denote significant differences (p < 0.05), as determined by paired *t*-test.

formation of some acidic substances. For example, acidic H_3O^+ ions can be formed from the reaction between water molecules and H_2O_2 generated by ACP, and HNO_3 and HNO_2 can be generated from NO through NO_2 (Ji et al., 2018). Because the inherent minerals of pea protein caused relatively low salt levels in suspension, the protein molecules aggregated in an ordered 'string-of-beads' via the weakened electrostatic repulsion after ACP treatment and possible attractive hydrophobic interactions between protein molecules (Bryant & McClements, 1998).

On the one hand, protein unfolding can expose free −SH groups that are originally hidden inside the protein globular structure, on the other hand, −SH groups are easily oxidized by reactive oxygen species (ROS) generated by ACP, such as ·OH (Zhang et al., 2020) and H_2O_2 (Sullivan & Sebranek, 2012). Thus, the changes of the total and exposed –SH groups, as well as the free −NH_2 groups of PPC before or after ACP treatment were measured and the results are displayed in Table 2. ACP treatment reduced the total −SH groups from 10.22 to 8.28 μmol/g protein. This was also observed in peanut protein and squid mantle protein after cold plasma treatment (Ji et al., 2018). However, the content of exposed free −SH groups was slightly increased after ACP treatment. These results suggest protein unfolding to expose more −SH groups, although the generated free −SH groups reacted with reactive species to form −S−S− bonds at the same time. Meanwhile, the free −NH_2 groups of PPC had no significant changes after ACP treating, which means no significant protein hydrolysis occurred.

Table 2
The contents of free −SH and −NH$_2$ groups of pea protein concentrate (PPC) suspensions with or without atmospheric cold plasma (ACP) treatment (3500 Hz, 10 μs, 10 min, 0–30 kV, and 0–1 A).

Samples	Free -SH contents (μmol/g protein)		Free -NH$_2$ contents (μmol -NH$_2$/mg protein)
	Total	Exposed	
PPC suspension	10.22 ± 0.03[b]	3.93 ± 0.03[a]	0.59 ± 0.02[a]
ACP-treated PPC suspension	8.28 ± 0.02[a]	4.07 ± 0.04[b]	0.61 ± 0.03[a]

Different lower-case letters within the same column denote significant differences (p < 0.05), as determined by paired *t*-test.

3.2.3. Protein conformation changes and surface hydrophobicity

The tertiary structure of proteins can be evaluated by studying intrinsic fluorescence spectra from tryptophan, tyrosine, and phenylalanine residues. Tryptophan residue is sensitive to the environment and has maximum fluorescence intensity, so it has been widely used as a measure of polarity and conformation changes of proteins (Chizoba Ekezie, Cheng, & Sun, 2018). Tryptophan residue has a high fluorescence intensity in the folded state when it is located in a hydrophobic environment of the protein (Cao & Xiong, 2015). But once the protein is denatured or unfolded, tryptophan residue is exposed to the solvent environment, resulting in the changes of fluorescence intensity. Fig. 5A shows the tryptophan fluorescence spectra of PPC with or without ACP treatment. The native PPC showed the maximum fluorescence emission spectrum of the tryptophan residue in the wavelength of near 340 nm. After ACP treatment, the fluorescence intensity decreased significantly, indicating the unfolding of PPC exposed tryptophan to a more hydrophilic environment. It is also possible that tryptophan oxidation occurred during ACP treatment because the hydrogen atom on the tryptophan indole ring could be removed by radicals. A study by Zhang et al. (2020) found that the fluorescence intensity of pork myofibrillar proteins decreased with increasing H$_2$O$_2$ concentration due to oxidation.

The protein surface hydrophobicity (H$_0$) was also determined to assess the protein denaturation. The H$_0$ value of PPC suspension increased from 19,800 to 23,000 after ACP treatment (Fig. 5B), indicating a higher number of ANS binding sites on the PPC surface. But the H$_0$ didn't increase too much, indicating PPC was only partially unfolded as a result of ACP treatment. Protein oxidation can lead to protein unfolding and denaturation with increased H$_0$, which might be caused by free radicals that broke the hydrogen bonds or electrostatic interactions in protein molecules (W. Sun, Zhao, Yang, Zhao, & Cui, 2011). Zhang et al. (2020) found a significant increase in H$_0$ of myofibrillar

proteins from pork muscle exposed to H$_2$O$_2$. Similar result was observed when the myofibrillar proteins were exposed to hydroxyl radicals (Zhang et al., 2020). Therefore, it is speculated that the increase in H$_0$ of ACP-treated PPC suspension could be caused by oxidation. The exposure of hydrophobic residues was favorable for the formation of the gel network through hydrophobic interactions.
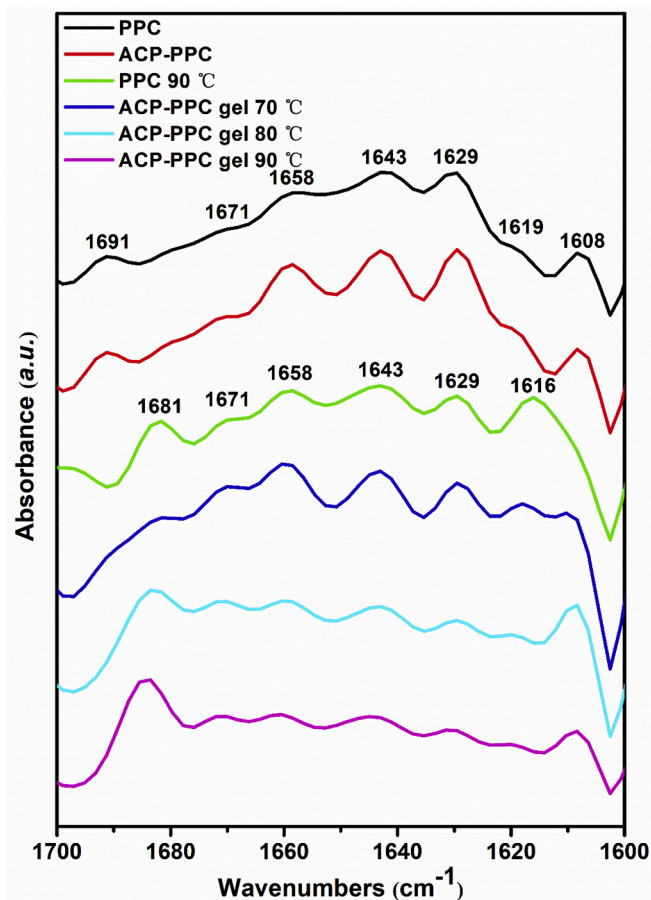

Fig. 6. Deconvoluted Fourier-transform infrared (FTIR) spectra of the amide I band (1600–1700 cm^{-1}) of untreated and ACP-treated pea protein concentrate (PPC) suspensions (12 wt%) and gels using ACP-treated PPC suspension (Treated conditions: 3500 Hz, 10 μs, 10 min, 0–30 kV, and 0–1 A) formed at 70, 80, and 90 °C for 30 min, respectively.
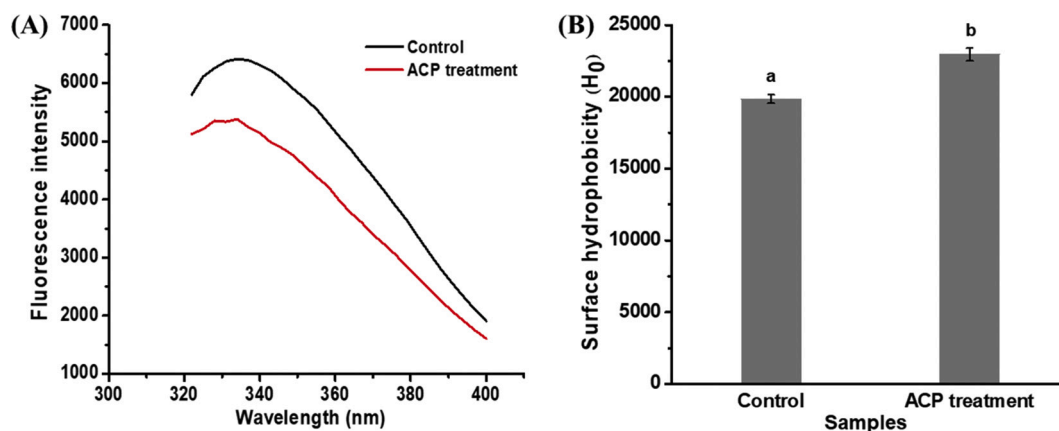

Fig. 5. Effect of atmospheric cold plasma (ACP) treatment (3500 Hz, 10 μs, 10 min, 0–30 kV, and 0–1 A) on the tertiary structure of pea protein concentrate (PPC). (A) Fluorescence intensity of PPC suspensions with or without ACP treatment. (B) Surface hydrophobicity (H$_0$) of PPC suspensions with or without ACP treatment. Different lower-case letters within a column denote significant differences (p < 0.05).

The changes in protein secondary structure were studied by FTIR through the analysis of the amide I band (1600–1700 cm^{-1}) (Fig. 6). Based on previous reports (Schmidt, Giacomelli, & Soldi, 2005; K. Wang & Arntfield, 2014), the bands were assigned to different protein secondary structures as follows: 1646–1664 cm^{-1} corresponded to α-helix, 1615–1637 and 1682–1700 cm^{-1} to β-sheet, 1664–1681 cm^{-1} to β-turn, and 1637–1645 cm^{-1} to random coils. After ACP treatment, the absorption of PPC still showed all the major secondary structure components, but the absorption intensity increased, especially for α-helix at 1658 cm^{-1} and β-sheet at 1629 cm^{-1}. This result indicates some reorganization of the PPC secondary structures, but no obvious protein unfolding was observed by ACP treatment.

Heating of the native PPC suspension at 90 °C for 30 min only partially unfolded pea protein due to its high denaturation temperature. Heating of ACP treated PPC at 70 °C did not lead to significant protein denaturation either, but interestingly a self-standing gel was able to be formed. When heating ACP-treated PPC at 80 and 90 °C, obvious protein denaturation was observed as reflected by the disappearance of the major protein secondary structural components. This was also accompanied by significant increase of the absorptions at 1691 and 1608 cm^{-1}, suggesting pea protein aggregation after unfolding. The band of at 1619 cm^{-1} corresponded to intermolecular β-sheets caused by aggregation via hydrogen bonds (Clark, Saunderson, & Suggett, 1981), while the one at 1691 cm^{-1} indicated the antiparallel β-sheets (Byler & Susi, 1986). This result indicates that ACP treatment enabled pea protein denaturation at reduced temperature of (80–90 °C) to facilitate protein interaction development for gel formation.

3.3. Gel formation mechanisms discussion

According to the above results, the possible gelling mechanism of atmospheric cold plasma (ACP) enabled pea protein gelation at reduced temperature is illustrated in Fig. 7. ACP treatment did not result in a significant change in the secondary structure of pea protein, but the protein tertiary structure partially unfolding, exposing the internal hydrophobic side chains and active sites. Then these active groups on the surface of protein molecules (such as –SH groups) might react with some free radicals generated by ACP to form covalent bonds (e.g., –S–S– bonds). At the same time, the ACP-treated pea protein concentrate (PPC) suspension contained a significant amount of negative charge, which prevented protein random aggregation, thus they grew linearly based on hydrophobic patches (Bryant, et al., 1998) to form fibrillar aggregates.

Subsequently, the ACP-treated PPC suspension was heated at 70, 80, and 90 °C for 30 min to induce gelation, followed by cooling to strengthen the gel network. Since the heating temperature of 70 °C did not significantly unfold the pea protein, undenatured protein formed particulate aggregates to build up a coarse and particulate network together with the initially formed fibrillar aggregates by ACP treatment, leading to self-standing but relatively weak gels (the compressive strength of 0.53 kPa). When the heating temperature reached 80 °C, the ACP treated pea protein was unfolded to develop a strong fibrillar network mainly stabilized by hydrogen bonding together with other interactions. This resulted in a gel with a compressive strength of 2.70 kPa, a water holding capacity of 85%, and good viscoelasticity. At a higher heating temperature of 90 °C, a stronger gel with a more homogenous porous structure was formed because the more fully unfolded protein exposed more hydrophobic groups and active sites. In this way, protein chains were crosslinked to the fibrillar aggregates formed by ACP treatment through more interactions. The gel strength could reach to 6.27 kPa, water holding capacity was 88%, and it showed good viscoelasticity.

To scale-up ACP technology, technical and economic challenges need to be addressed (Feizollahi et al., 2020). ACP has the potential to improve the gelling properties of pea protein. Process and product parameters including but not limited to, ACP treatment time, type of gas to generate ACP, power, frequency, voltage, and water content should be optimized in order to develop a cost-effective ACP process for improving the gelling properties of pea protein and other plant based proteins. It is difficult to control and monitor the plasma chemistry and uniformity in a large scale due to the complex nature of the reactive species generated by ACP. Thus, it is necessary to design and develop ACP equipment systems with large treatment area and uniform distribution of plasma to
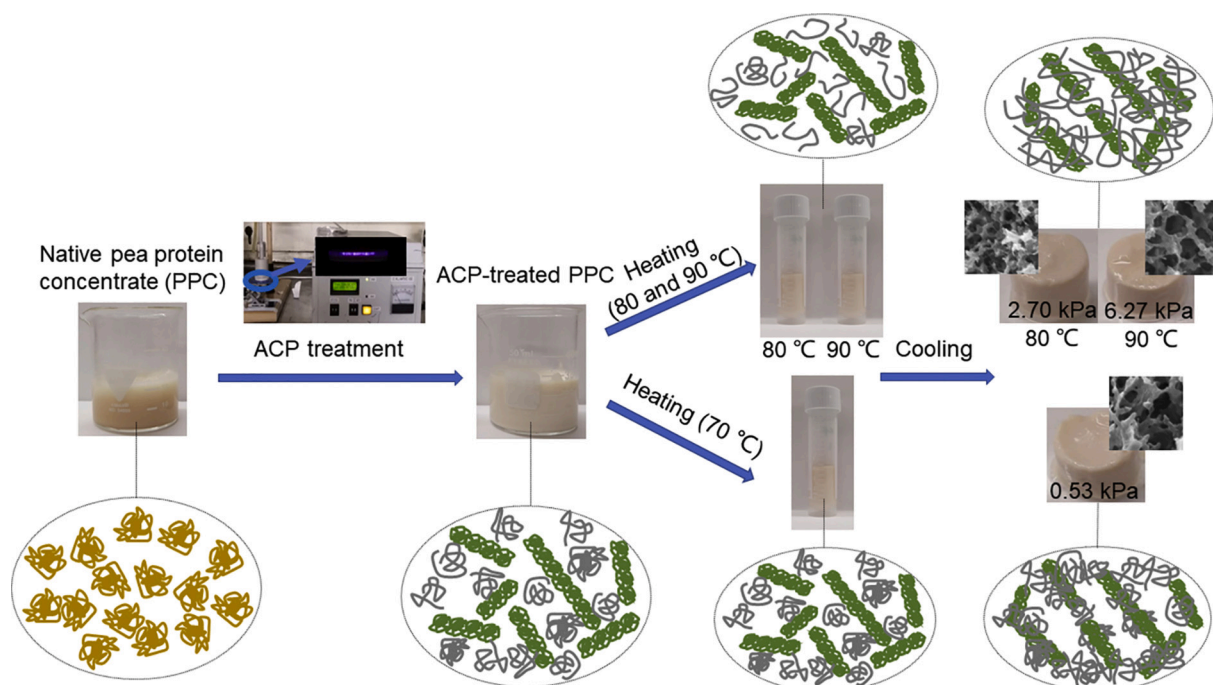

Fig. 7. Schematic illustration of the gelling mechanism of atmospheric cold plasma (ACP) enabled pea protein gelation at reduced temperatures (70, 80, and 90 °C). The yellow represents the native pea protein, the green represents the aggregates formed after ACP treatment, and the grey represents the protein molecules with secondary and/or tertiary structure unfolded.

expand it from laboratory research to food industry. Future research also should focus on ACP process validation to ensure the safety and quality of the final products (Feizollahi et al., 2020).

4. Conclusions

This is the first study to reveal that ACP treatment enabled pea protein denaturation at reduced temperature (70–90 °C) to improve its gelling properties. While native pea protein concentrate (PPC) (12 wt%) did not form a self-standing gel at 90 °C, PPC after ACP treatment did form strong and elastic gels by heating at 80–90 °C through hydrogen bonding and other interactions. In addition, the gels demonstrated high water holding capacity. This study not only provides a new method to develop PPC gels but expands the application of ACP technology for food applications. In light of the short treatment time, reduced gelling temperature, and low protein concentration, the gel prepared by heating ACP-treated pea protein at 80–90 °C for 30 min has the potential for the development of meat binders, fat replacers, and meat analogues in food industry. The oxidation mechanism of ACP on pea protein and specific effects of aggregates formed during ACP treatment on protein gel properties should be further studied to develop a theoretical basis for predicting the functional properties of ACP treated pea proteins.

CRediT authorship contribution statement

Sitian Zhang: Conceptualization, Methodology, Validation, Writing - original draft. **Weijuan Huang:** Conceptualization, Methodology, Writing - review & editing. **Ehsan Feizollahi:** Methodology, Writing - review & editing. **M.S. Roopesh:** Resources, Writing - review & editing, Project administration. **Lingyun Chen:** Conceptualization, Resources, Writing - review & editing, Supervision, Project administration, Funding acquisition.

Declaration of Competing Interest

The authors declare no conflicts of interest.

Acknowledgements

References

DHHS. (2017). Food safety when cooking. https://www.betterhealth.vic.gov.au/health/healthyliving/food-safety-when-cooking.

Abaee, A., Mohammadian, M., & Jafari, S. M. (2017). Whey and soy protein-based hydrogels and nano-hydrogels as bioactive delivery systems. *Trends in Food Science & Technology, 70*, 69–81. https://doi.org/10.1016/j.tifs.2017.10.011

Bahrami, N., Bayliss, D., Chope, G., Penson, S., Perehinec, T., & Fisk, I. D. (2016). Cold plasma: A new technology to modify wheat flour functionality. *Food Chemistry, 202*, 247–253. https://doi.org/10.1016/j.foodchem.2016.01.113

Bard, D. (2019). Update on Canada's pulse crops. https://pulsepod.globalpulses.com/pod-feed/post/update-on-canada-pulse-crops.

Ben-Harb, S., Panouillé, M., Huc-Mathis, D., Moulin, G., Saint-Eve, A., Irlinger, F., Bonnarme, P., Michon, C., & Souchon, I. (2018). The rheological and microstructural properties of pea, milk, mixed pea/milk gels and gelled emulsions designed by thermal, acid, and enzyme treatments. *Food Hydrocolloids, 77*, 75–84. https://doi.org/10.1016/j.foodhyd.2017.09.022

Braga, A. L. M., Azevedo, A., Marques, M. J., Menossi, M., & Cunha, R. L. (2006). Interactions between soy protein isolate and xanthan in heat-induced gels: The effect of salt addition. *Food Hydrocolloids, 20*(8), 1178–1189. https://doi.org/10.1016/j.foodhyd.2006.01.003

Brito-Oliveira, T. C., Bispo, M., Moraes, I. C., Campanella, O. H., & Pinho, S. C. (2018). Cold-set gelation of commercial soy protein isolate: Effects of the incorporation of

locust bean gum and solid lipid microparticles on the properties of gels. *Food Biophysics, 13*(3), 226–239. https://doi.org/10.1007/s11483-018-9529-4

Bryant, C. M., & McClements, D. J. (1998). Molecular basis of protein functionality with special consideration of cold-set gels derived from heat-denatured whey. *Trends in Food Science & Technology, 9*(4), 143–151. https://doi.org/10.1016/S0924-2244(98)00031-4

Bußler, S., Steins, V., Ehlbeck, J., & Schlüter, O. (2015). Impact of thermal treatment versus cold atmospheric plasma processing on the techno-functional protein properties from Pisum sativum 'Salamanca'. *Journal of Food Engineering, 167*, 166–174. https://doi.org/10.1016/j.jfoodeng.2015.05.036

Cao, Y., & Xiong, Y. L. (2015). Chlorogenic acid-mediated gel formation of oxidatively stressed myofibrillar protein. *Food Chemistry, 180*, 235–243. https://doi.org/10.1016/j.foodchem.2015.02.036

Chalamaiah, M., Esparza, Y., Temelli, F., & Wu, J. (2017). Physicochemical and functional properties of livetins fraction from hen egg yolk. *Food Bioscience, 18*, 38–45. https://doi.org/10.1016/j.fbio.2017.04.002

Chizoba Ekezie, F.-G., Cheng, J.-H., & Sun, D.-W. (2018). Effects of mild oxidative and structural modifications induced by argon plasma on physicochemical properties of Actomyosin from king prawn (Litopenaeus vannamei). *Journal of Agricultural and Food Chemistry, 66*(50), 13285–13294. https://doi.org/10.1021/acs.jafc.8b05178

Croy, R., Gatehouse, J. A., Tyler, M., & Boulter, D. (1980). The purification and characterization of a third storage protein (convicilin) from the seeds of pea (Pisum sativum L.). *Biochemical Journal, 191*(2), 509–516. https://doi.org/10.1042/bj1910509

Deng, S., Ruan, R., Mok, C. K., Huang, G., Lin, X., & Chen, P. (2007). Inactivation of Escherichia coli on almonds using nonthermal plasma. *Journal of Food Science, 72*(2), M62–M66. https://doi.org/10.1111/j.1750-3841.2007.00275.x

Dong, S., Gao, A., Xu, H., & Chen, Y. (2017). Effects of dielectric barrier discharges (DBD) cold plasma treatment on physicochemical and structural properties of zein powders. *Food and Bioprocess Technology, 10*(3), 434–444. https://doi.org/10.1007/s11947-017-2015-z

Dong, S., Guo, P., Chen, Y., Chen, G.-Y., Ji, H., Ran, Y., … Chen, Y. (2018). Surface modification via atmospheric cold plasma (ACP): Improved functional properties and characterization of zein film. *Industrial Crops and Products, 115*, 124–133. https://doi.org/10.1016/j.indcrop.2018.01.080

Dong, S., Wang, J.-M., Cheng, L.-M., Lu, Y.-L., Li, S.-H., & Chen, Y. (2017). Behavior of zein in aqueous ethanol under atmospheric pressure cold plasma treatment. *Journal of Agricultural and Food Chemistry, 65*(34), 7352–7360. https://doi.org/10.1021/acs.jafc.7b02205

Feizollahi, E., Misra, N., & Roopesh, M. (2020). Factors influencing the antimicrobial efficacy of dielectric barrier discharge (DBD) atmospheric cold plasma (ACP) in food processing applications. *Critical Reviews in Food Science and Nutrition*, 1–24. https://doi.org/10.1080/10408398.2020.1743967

Fujihara, S., Kasuga, A., & Aoyagi, Y. (2001). Nitrogen-to-protein conversion factors for common vegetables in Japan. *Journal of Food Science, 66*(3), 412–415. https://doi.org/10.1111/j.1365-2621.2001.tb16119.x

Habeeb, A. S. A. (1966). Determination of free amino groups in proteins by trinitrobenzenesulfonic acid. *Analytical Biochemistry, 14*(3), 328–336. https://doi.org/10.1016/0003-2697(66)90275-2

Ji, H., Dong, S., Han, F., Li, Y., Chen, G., Li, L., & Chen, Y. (2018). Effects of dielectric barrier discharge (DBD) cold plasma treatment on physicochemical and functional properties of peanut protein. *Food and Bioprocess Technology, 11*(2), 344–354. https://doi.org/10.1007/s11947-017-2015-z

Ji, H., Han, F., Peng, S., Yu, J., Li, L., Liu, Y., … Chen, Y. (2019). Behavioral Solubilization of Peanut protein isolate by atmospheric pressure cold plasma (ACP) treatment. *Food and Bioprocess Technology, 12*(12), 2018–2027. https://doi.org/10.1007/s11947-019-02357-0

Kato, A., & Nakai, S. (1980). Hydrophobicity determined by a fluorescence probe method and its correlation with surface properties of proteins. *Biochimica et biophysica acta (BBA)-Protein structure, 624*(1), 13–20. https://doi.org/10.1016/0005-2795(80)90220-2

Kim, J. E., Lee, D.-U., & Min, S. C. (2014). Microbial decontamination of red pepper powder by cold plasma. *Food Microbiology, 38*, 128–136. https://doi.org/10.1016/j.fm.2013.08.019

Liang, H.-N., & Tang, C.-H. (2013). pH-dependent emulsifying properties of pea [Pisum sativum (L.)] proteins. *Food Hydrocolloids, 33*(2), 309–319. https://doi.org/10.1016/j.foodhyd.2013.04.005

Mandal, R., Singh, A., & Singh, A. P. (2018). Recent developments in cold plasma decontamination technology in the food industry. *Trends in Food Science & Technology, 80*, 93–103. https://doi.org/10.1016/j.tifs.2018.07.014

Martínez-López, A. L., Carvajal-Millan, E., Micard, V., Rascón-Chu, A., Brown-Bojorquez, F., Sotelo-Cruz, N., … Lizardi-Mendoza, J. (2016). In vitro degradation of covalently cross-linked arabinoxylan hydrogels by bifidobacteria. *Carbohydrate Polymers, 144*, 76–82. https://doi.org/10.1016/j.carbpol.2016.02.031

Miao, W., Nyaisaba, B. M., Koddy, J. K., Chen, M., Hatab, S., & Deng, S. (2020). Effect of cold atmospheric plasma on the physicochemical and functional properties of myofibrillar protein from Alaska Pollock (Theragra chalcogramma). *International Journal of Food Science & Technology, 55*(2), 517–525. https://doi.org/10.1111/ijfs.14295

Moreno, H. M., Domínguez-Timón, F., Díaz, M. T., Pedrosa, M. M., Borderías, A. J., & Tovar, C. A. (2020). Evaluation of gels made with different commercial pea protein isolate: Rheological, structural and functional properties. *Food Hydrocolloids, 99*, 105375. https://doi.org/10.1016/j.foodhyd.2019.105375

Munialo, C. D., van der Linden, E., & de Jongh, H. H. (2014). The ability to store energy in pea protein gels is set by network dimensions smaller than 50 nm. *Food Research International, 64*, 482–491. https://doi.org/10.1016/j.foodres.2014.07.038

Nieto-Nieto, T. V., Wang, Y. X., Ozimek, L., & Chen, L. (2015). Inulin at low concentrations significantly improves the gelling properties of oat protein–a molecular mechanism study. *Food Hydrocolloids, 50,* 116–127. https://doi.org/10.1016/j.foodhyd.2015.03.031

Nieto-Nieto, T. V., Wang, Y., Ozimek, L., & Chen, L. (2016). Improved thermal gelation of oat protein with the formation of controlled phase-separated networks using dextrin and carrageenan polysaccharides. *Food Research International, 82,* 95–103. https://doi.org/10.1016/j.foodres.2016.01.027

O'Kane, F. E., Vereijken, J. M., Gruppen, H., & Van Boekel, M. A. (2005). Gelation behavior of protein isolates extracted from 5 cultivars of Pisum sativum L. *Journal of Food Science, 70*(2), C132–C137. https://doi.org/10.1111/j.1365-2621.2005.tb07073.x

Picout, D. R., & Ross-Murphy, S. B. (2003). Rheology of biopolymer solutions and gels. *The Scientific World Journal, 3,* 105–121. https://doi.org/10.1100/tsw.2003.15

Schmidt, V., Giacomelli, C., & Soldi, V. (2005). Thermal stability of films formed by soy protein isolate–sodium dodecyl sulfate. *Polymer Degradation and Stability, 87*(1), 25–31. https://doi.org/10.1016/j.polymdegradstab.2004.07.003

Shand, P., Ya, H., Pietrasik, Z., & Wanasundara, P. (2007). Physicochemical and textural properties of heat-induced pea protein isolate gels. *Food Chemistry, 102*(4), 1119–1130. https://doi.org/10.1016/j.foodchem.2006.06.060

Sullivan, G. A., & Sebranek, J. G. (2012). Nitrosylation of myoglobin and nitrosation of cysteine by nitrite in a model system simulating meat curing. *Journal of Agricultural and Food Chemistry, 60*(7), 1748–1754. https://doi.org/10.1021/jf204717v

Sun, W., Cui, C., Zhao, M., Zhao, Q., & Yang, B. (2011). Effects of composition and oxidation of proteins on their solubility, aggregation and proteolytic susceptibility during processing of Cantonese sausage. *Food Chemistry, 124*(1), 336–341. https://doi.org/10.1016/j.foodchem.2010.06.042

Tayeh, N., Aubert, G., Pilet-Nayel, M.-L., Lejeune-Hénaut, I., Warkentin, T. D., & Burstin, J. (2015). Genomic tools in pea breeding programs: Status and perspectives. *Frontiers in Plant Science, 6,* 1037. https://doi.org/10.3389/fpls.2015.01037

Tsumura, K., Saito, T., Tsuge, K., Ashida, H., Kugimiya, W., & Inouye, K. (2005). Functional properties of soy protein hydrolysates obtained by selective proteolysis. *LWT-Food Science and Technology, 38*(3), 255–261. https://doi.org/10.1016/j.lwt.2004.06.007

Walia, N., & Chen, L. (2020). Pea protein based vitamin D nanoemulsions: Fabrication, stability and in vitro study using Caco-2 cells. *Food Chemistry, 305,* 125475. https://doi.org/10.1016/j.foodchem.2019.125475

Wang, K., & Arntfield, S. D. (2014). Binding of carbonyl flavours to canola, pea and wheat proteins using GC/MS approach. *Food Chemistry, 157,* 364–372. https://doi.org/10.1016/j.foodchem.2014.02.042

Wang, K.-Q., Luo, S.-Z., Zhong, X.-Y., Cai, J., Jiang, S.-T., & Zheng, Z. (2017). Changes in chemical interactions and protein conformation during heat-induced wheat gluten gel formation. *Food Chemistry, 214,* 393–399. https://doi.org/10.1016/j.foodchem.2016.07.037

Wu, M., Xiong, Y. L., Chen, J., Tang, X., & Zhou, G. (2009). Rheological and microstructural properties of porcine myofibrillar protein–lipid emulsion composite gels. *Journal of Food Science, 74*(4), E207–E217. https://doi.org/10.1111/j.1750-3841.2009.01140.x

Yang, C., Wang, Y., Vasanthan, T., & Chen, L. (2014). Impacts of pH and heating temperature on formation mechanisms and properties of thermally induced canola protein gels. *Food Hydrocolloids, 40,* 225–236. https://doi.org/10.1016/j.foodhyd.2014.03.011

Zhang, D., Li, H., Emara, A., Hu, Y., Wang, Z., Wang, M., & He, Z. (2020). Effect of in vitro oxidation on the water retention mechanism of myofibrillar proteins gel from pork muscles. *Food Chemistry, 315,* 126226. https://doi.org/10.1016/j.foodchem.2020.126226